An Imager using 2-D Single-Photon Avalanche Diode Array in 0.18-μm CMOS for Automotive LIDAR Application *

Hironobu AKITA　Isamu TAKAI　Kenta AZUMA
Takehiro HATA　Noriyuki OZAKI

A feasibility imager chip of a 32 x 4-pixel array was developed in a 0.18-μ m CMOS process for a small size automotive laser imaging detection and ranging. Each pixel consists of 8 single-photon avalanche diodes as a world-first 2-D pixel array with digital output macro pixel architecture which enables laser signal sensing under sunlight noise. Distance measurement results show less than 2.1% nonlinearity and 0.11-m standard deviation up to 20-m distance with 10%-reflective target under the ambient light of 75 klux.

Key words :
LIDAR, ToF, SPAD, Macro pixel, imager, avalanche, ADAS, autonomous driving

Introduction

The progress of advanced driver assistant systems (ADAS) and/or autonomous driving (AD) cars can reduce traffic accidents significantly and save vulnerable road users' lives[1) 2)]. In addition to the camera and the millimeter-wave radar currently employed for the surround vehicle sensing, a laser imaging detection and ranging (LIDAR), is expected to offer the precise distance and spatial resolution by the time-of-flight (ToF) measurements[3)].

The mechanism of the raging sensor is illustrated in Fig. 1. The transmitter emits the signal to the object, and the receiver detects the return signal with measuring the travelling time of the signal. Since this time is proportional to the distance, the sensor can detect the distance to the object as well as the existence of the object itself. The angular resolution and/or accuracy are affected by the signal beam divergence. The light has superior divergence characteristics compared with the ultrasound or the radio wave due to its higher frequency, thus shorter wavelength. As shown in Fig. 2, LIDAR has the higher signal frequency than other ranging sensors. Therefore, it is a suitable technology for the high resolution raging sensor.

LIDARs equipped with a mechanical rotating mirror[4)] or a self-spinning mechanism[5)] has ever been developed to scan sensing directions. Furthermore, from the viewpoint of reliability and downsizing, we have also developed the small size LIDAR composed of a micro electro mechanical systems (MEMS) based scanner and a 2-D pixel array[6)].

* IEEE の許可を得て Symposium on VLSI Circuits 2017, C22-2 より一部改版して転載

In this paper, we report the feasibility of a single-photon avalanche diode (SPAD) based 2-D pixel array designed with a macro pixel architecture for the ambient light noise suppression, which has been adopted for the 1-D SPAD-based pixel array[4].

Fig. 1 Mechanism of the ranging sensor

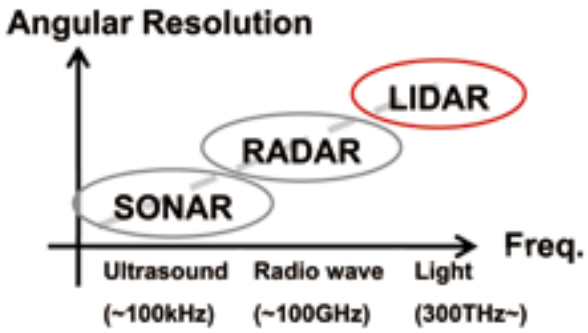

Fig. 2 Angular esolution dependency on the signal frequency

SPAD and Macro Pixel Architecture

We have developed the SPAD with enhanced near-infrared sensitivity for the LIDAR[7]. The SPAD is a PN junction diode biased with the reversely higher voltage than PD (photo diode) or APD (avalanche photo diode) as shown in Fig. 3. Since the biased voltage is much higher than its breakdown voltage, the SPAD can detect even a single photon. On detecting an incident photon, the SPAD output a voltage pulse generated by an avalanche breakdown current and a quenching resistor. The duration of this pulse, known as 'dead time', highly affects the performance of the SPAD since it can be paralyzed by the consecutive photons, especially under the ambient sunlight condition. The macro pixel architectures have been proposed to conceal the dead time, in which each pixel comprises several SPADs and exploits the spatial and temporal correlation of the incident photons[4]. When the same area of one pixel is divided into N SPADs, the average output pulse rate λout from this pixel can be expressed theoretically as:

$$\lambda out = (Pin \times PDE \times FF + \lambda dark) \times \exp\left(-\frac{Pin \times PDE \times FF + \lambda dark}{N} \times \tau d\right),$$

where Pin and $\lambda dark$ represent the average rates of the input incident photon and the dark count, respectively. PDE, FF, and τd are the photon detection efficiency, the fill factor, and the dead time[8]. The output pulse rates, depicted in Fig. 4, are the calculated results with the same pixel size, which is divided into the various numbers of SPADs. It shows the behavior of saturation and drop at the high incident photon rate due to the dead time, and it limits the maximum of the output dynamic rage. A noise floor is determined by the incident photons' rate of the ambient sunlight for the automotive LIDAR. In the case of the pixel with one SPAD, the noise floor reaches the maximum limit at the condition of 75 klux sunlight as shown in Fig. 4, and therefore no additional photons by the reflected laser can be sensed any more. This can be mitigated by increasing the number of divided SPADs. In the case of 8 SPADs/pixel, dynamic range can be improved by one decade. Although this architecture requires many SPADs for the 2-D array, it will become applicable, owing to the progress of the LSI process technology. Now, large CMOS imager chips with the active image area as full or super 35-mm format have developed[9], which will be available in the near future for the SPAD-based imager. If we assign horizontal 640 pixels of VGA on a 27-mm length of the active area, the pixel becomes 42-μm pitch, and with our 20-μm pitch SPAD, the macro pixel of 2 × 4 SPAD arrangements can be realized.

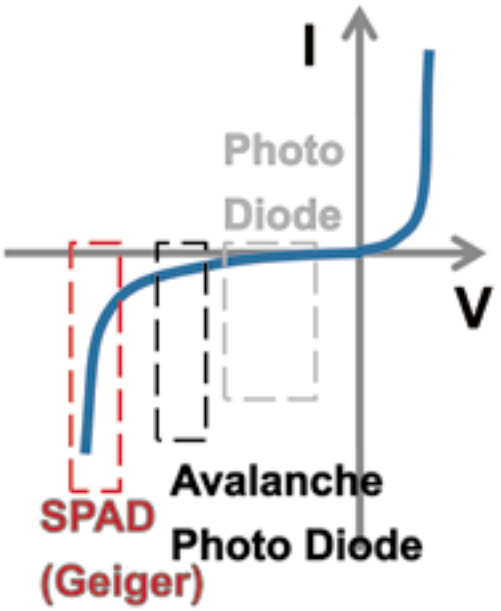

Fig. 3 SPAD operation point

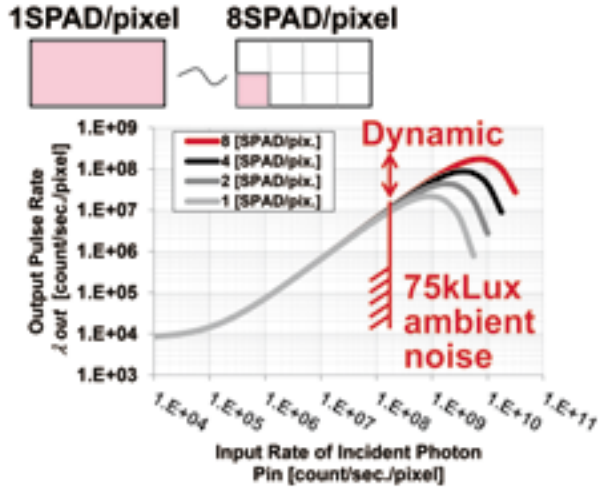

Fig. 4 Output pulse rate characteristics depending on the division number *N* in the macro pixel

Chip Design and Measurement Results

A block diagram of the imager is shown in Fig. 5. Each macro pixel, composing a 32 × 4 pixel array, is consisting of 8 SPADs as the macro pixel architecture. Each SPAD is connected to its adjacent front-end circuit including the quenching resistor, the AC-coupled addressing gate, and open drain buffer to share the data line among the SPADs in the same row. The SPADs' output pulses from two columns of the same pixel are selected by the address decoder simultaneously, and are, as digital signals, fed to a correlation detection circuit, which detects and passes only the incoming pulses from simultaneous two or more photons' events, yet blocking single photon's events to suppress the noise. Upon the detection, the ToF is counted by a time-to-digital converter (TDC) with 208 psec. resolution, and the peak number of simultaneous pulses is stored in a memory, accumulating at the address of the measured ToF for 10 cycles. By reading out the contents in the memory externally, the histogram of ToF can be obtained.

A Photomicrograph of the fabricated chip is shown in Fig. 6, implemented in a 0.18-μm CMOS image sensor technology. The SPAD's active junction is shown in the inset including the front-end circuits. The fill factor of the SPAD is 28% based on the layout. Each macro pixel and the TDC are connected in the longitudinal direction, considering the number of the data line shared by the SPADs of the same pixel. Even though the length varies almost up to 2 mm between the nearest and farthest pixels, the variance of the signal propagation delay is adjusted to be less than the resolution of the TDC by the careful parasitic extraction and layout iterations.

The chip is evaluated with an 870-nm laser of 46 W and 4-nsec pulse width, combining with the MEMS scanner and optical lenses. Distance measurements are performed inside our laboratory with artificial sunlight as the ambient light noise source. The performances are confirmed as 2.1% accuracy and 0.11-m standard deviation as shown in Fig. 7 (a) and Fig. 7 (b), respectively, for up to 20-m distance with the target of 10% reflectivity under ambient light of 75 klux.

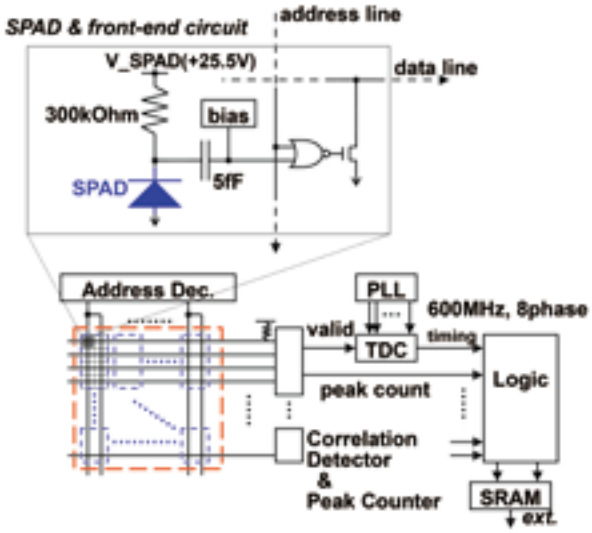

Fig. 5 Block diagram of the imager chip

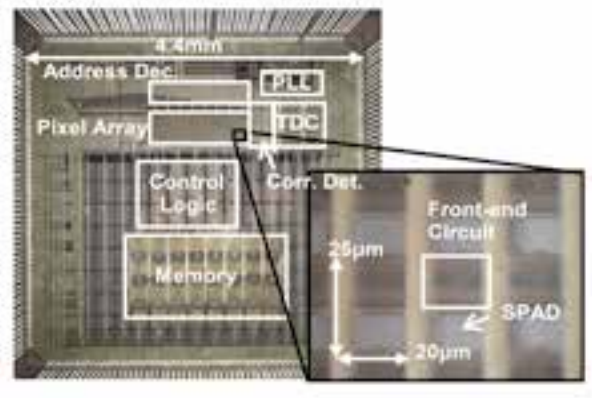

Fig. 6 Photomicrograph of a fabricated chip with magnified SPADs in the inset

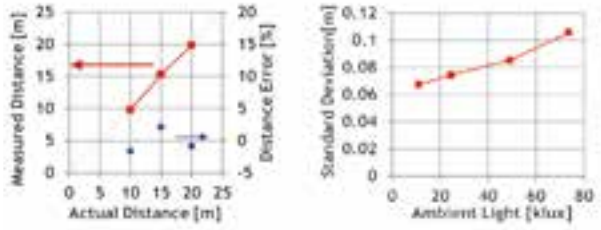

(a) (b)

Fig. 7 Measurement results. (a) Distance and its error. (b) Ambient-light dependency. Deviations are calculated from the data of 300-cycles repetition. Both measurements are done with the lens of F number 2.0 and focal length 8.2 mm

Table 1 Comparison with prior works

	[4]	[5]	[6]	This Work
Pixel Arrange	1D Array	Discrete PD Array	2D Array	2D Array
Macro Pixel Architecture	Yes (12SPAD/Pixel)	No	No	Yes (8SPAD/Pixel)
Scanner (Size**)	Motor + Mirror (100cc)	Motor +Spin Module (200cc)	MEMS (2cc)	MEMS (2cc)
Max. Distance	40m	100m~	25m	20m
Target Reflectivity	9%	----	white	10%
Ambient Light	80klux	----	10klux	75klux

** Rough approximation

Summary and Future Work

The feasibility of the macro pixel architecture applied on a 2-D SPAD-based pixel array is demonstrated by the fabricated imager chip in a 0.18-μm CMOS. From measurement results, the distance measurement operation is confirmed up to 20 m under the ambient light noise of 75 klux. Table 1 compares our work with the published technologies. The higher sensitivity under the ambient light noise condition is achieved with the 2-D pixel array which enables the usage of the MEMS scanner and realizes the small size automotive LIDAR.

From the viewpoint of the chip area efficiency, on the contrary, the layout shrinkage by adopting the fine pitch processes is desirable for the peripheral circuits. Since these processes are not compatible, generally, with the high voltage used for the SPAD, we will separate the SPAD array and peripheral circuits on the different process die. They will be stacked and connected with each other, for the next step.

Acknowledgement

The authors would like to thank S. Kashiwada, T. Kimura, and H. Matsubara for their valuable discussion, K. Yanai and K. Tsuruta for their support of this project. This paper is based on results obtained from a project commissioned by the New Energy and

Industrial Technology Development Organization (NEDO).

References

1) World Health Organization (WHO), "Global status report on road safety," 2015
2) J. D. Rupp, *et al.*, "Autonomous driving-A practical roadmap," SAE Tech. Paper, No. 2010-01-2335, 2010.
3) A. Bastian, *et al.*, "Autonomous cruise control: A first step towards automated driving," SAE Tech. Paper, No. 981942, 1998.
4) C. Niclass, *et al.*, "A 100-m Range 10-Frame/s 340 96-Pixel Time-of-Flight Depth Sensor in 0.18-μm CMOS." IEEE Journal of Solid-State Circuits 48.2, pp. 559-572, 2013.
5) B. Schwarz, "Mapping the world in 3D," Nature Photonics, 4.7, pp. 429-430, 2010.
6) K. Ito, *et al.*, "System design and performance characterization of a MEMS-based laser scanning time-of-flight sensor based on a 256 64-pixel single-photon imager," IEEE Photonics Journal, 5.2, No. 6800114, 2013.
7) I. Takai, *et al.*, "Single-Photon Avalanche Diode with Enhanced NIR-Sensitivity for Automotive LIDAR Systems." Sensors, 16.4, 459, 2016.
8) A. Eisele, *et al.*, "185 MHz count rate, 139 dB dynamic range single-photon avalanche diode with active quenching circuit in 130 nm CMOS technology," International Image Sensor Workshop, 2011.
9) R. Funatsu, *et al.*, "133Mpixel 60fps CMOS image sensor with 32-column shared high-speed column-parallel SAR ADCs," IEEE ISSCC Digest of Technical Papers, pp. 112-113, 2015.

著者

秋田 浩伸
あきた ひろのぶ

先進モビリティシステム開発部
LiDAR システムの研究に従事

高井 勇
たかい いさむ

㈱豊田中央研究所
システム・エレクトロニクス1部
博士 (工学)
高機能イメージセンサおよび LiDAR システムの研究に従事

東 謙太
あずま けんた

先進モビリティシステム開発部
LiDAR システムの研究に従事

秦 武廣
はた たけひろ

先進モビリティシステム開発部
LiDAR システムの研究に従事

尾崎 憲幸
おざき のりゆき

先進モビリティシステム開発部
LiDAR システムの研究に従事